Accessing unpolarized and linearly polarized gluon TMDs through quarkonium production

Asmita Mukherjee and Sangem Rajesh*
Department of Physics, Indian Institute of Technology Bombay, Mumbai-400076, India.
(Dated: January 3, 2017)

We present the study of accessing unpolarized and linearly polarized gluon TMDs in J/ψ and $\Upsilon(1S)$ production in unpolarized proton-proton collision at LHC, RHIC and AFTER energies. Non-relativistic QCD based color octet model (COM) is used for estimating quarkonium production rates within transverse momentum dependent factorization formalism. A comparison is drawn between the experimental data and the transverse momentum distribution of quarkonium obtained in COM and color evaporation model.

arXiv:1701.00329v1 [hep-ph] 2 Jan 2017

I. INTRODUCTION

Amongst the eight leading twist-2 transverse momentum dependent parton distribution functions (TMDs) [1, 2, 3], $f_1^g(x, \mathbf{k}_\perp)$ and $h_1^{\perp g}(x, \mathbf{k}_\perp)$ are the only two TMDs which describe the dynamics of gluons inside an unpolarized hadron while f_1^g and $h_1^{\perp g}$ represent the density of unpolarized and linearly polarized gluons inside an unpolarized hadron respectively. TMDs have been receiving paramount interest in both theoretically and experimentally as they provide the 3-dimensional structure and spin information of the nucleon. TMDs depend on both longitudinal momentum fraction (x) and intrinsic transverse momentum ($k_\perp$) of the parton whereas usual collinear parton distribution functions (PDFs) depend only on x. Gauge links are required to define the gauge invariant operator definition of TMDs and are process dependent.

In general, linearly polarized gluons can be present even at tree level inside an unpolarized hadron [1] provided that the gluons carry transverse momentum w.r.t parent hadron. The associated density function of linearly polarized gluons, $h_1^{\perp g}$ is a T-even (time-reversal even) distribution and is also even in the transverse momentum. TMDs are nonperturbative objects and have to be extracted from experiments. Drell-Yan (DY) and semi-inclusive deep inelastic scattering (SIDIS) are the two processes which provide the experimental data related to the TMDs [4]. In these processes, the intrinsic transverse momentum ($k_\perp$) has an imprint on the experimentally measurable quantities, for instance, azimuthal asymmetries and transverse momentum (p_T) distribution of the final hadron. Hence, these quantities are very sensitive to the TMDs. However, $h_1^{\perp g}$ and even f_1^g have not been extracted yet. Gluon Sivers function ($f_1^{\perp g}$) [5] generates single spin asymmetry in scattering processes like $ep^\uparrow$ and $pp^\uparrow$. In order to understand asymmetries fully, one should have complete knowledge about unpolarized TMDs since f_1^g sits in the denominator of the asymmetry expression [4]. Therefore, the extraction of f_1^g and $h_1^{\perp g}$ functions are of prime importance. In order to probe $h_1^{\perp g}$, several processes have been proposed theoretically. Linear gluon polarization can be determined by measuring azimuthal asymmetry in heavy quark pair and dijet production in SIDIS [6], $\Upsilon + jet$ [7] and $\gamma\gamma$ [8] in pp collision at LHC. $h_1^{\perp g}$ can also be accessed through the cross section of Higgs-boson [9, 10, 11, 12], Higgs+jet [13] and C-even (charge conjugation even) quarkonium production [14].

In this proceeding contribution, we discuss the J/ψ and $\Upsilon(1S)$ production in unpolarized proton-proton collision to show that the quarkonium production is also a promising channel to extract both f_1^g and $h_1^{\perp g}$. Details of our work can be found in [15, 16]. We estimate the quarkonium production rates using color octet model (COM) [15] within transverse momentum dependent (TMD) [17] framework and draw a comparison between the results with color evaporation model (CEM) [16] and experimental data. COM, color singlet model (CSM) and CEM are the three important models for quarkonium production, which are successful at different energies. Generally, two scales are involved in quarkonium production [18, 19, 20]. The first one is related to the production of heavy quark pair with momentum of order M (heavy quark mass) which is called short distance factor. This short distance factor can be calculated in order $\alpha_s(M)$ using perturbation theory. The second one is the binding of quarkonium bound state which is taking place at scale of order $\Lambda_{\rm QCD}$. This is a nonperturbative process and is denoted with long distance matrix elements (LDME) in factorization expression. The hadronization information is encoded in the LDME which are usually extracted by fitting data. The non-relativistic Quantum chromodynamics (NRQCD) effective field theory [20] separates the short distance and long distance factors systematically. In COM [21], the initially produced heavy quark pair can be either in color singlet or octet state.

II. J/ψ AND $\Upsilon(1S)$ PRODUCTION IN COM

We consider unpolarized proton-proton collision process for quarkonium production *i.e.*, $p + p \rightarrow J/\psi$ or $\Upsilon(1S) + X$. Proton is rich of gluons at high energy,

* This proceeding is based on a talk delivered at 22nd International Spin Symposium, 2016, UIUC.; rajeshphy@phy.iitb.ac.in

hence we consider the leading order (LO) gluon-gluon fusion channel for quarkonium production. Assuming that the TMD factorization holds good, the differential cross section is given by [15]

$$d\sigma = \int dx_a dx_b d^2\mathbf{k}_{\perp a} d^2\mathbf{k}_{\perp b} \Phi_g^{\mu\nu}(x_a, \mathbf{k}_{\perp a}) \times \Phi_{g\mu\nu}(x_b, \mathbf{k}_{\perp b}) d\sigma^{J/\psi(\Upsilon)}, \quad (1)$$

where, $\Phi_g^{\mu\nu}$ is the gluon-gluon correlator of unpolarized spin-$\frac{1}{2}$ hadron, which can be further parametrized in terms of leading twist-2 TMDs as the following [1]

$$\Phi_g^{\mu\nu}(x, \mathbf{k}_\perp) = -\frac{1}{2x}\Big\{g_T^{\mu\nu} f_1^g(x, \mathbf{k}_\perp^2) - \Big(\frac{k_\perp^\mu k_\perp^\nu}{M_h^2} + g_T^{\mu\nu}\frac{\mathbf{k}_\perp^2}{2M_h^2}\Big) h_1^{\perp g}(x, \mathbf{k}_\perp^2)\Big\}. \quad (2)$$

Here f_1^g and $h_1^{\perp g}$ are the unpolarized and linearly polarized gluon TMDs respectively. M_h is the proton mass. The $d\sigma^{J/\psi(\Upsilon)}$ in Eq.(1) is the partonic differential cross section of $gg \to Q\bar{Q}[^{2S+1}L_J^{(a)}]$ channel. Using NRQCD, the partonic differential cross section can be factorized as follows [20, 22]

$$d\sigma^{J/\psi(\Upsilon)} = \sum_n d\hat{\sigma}[gg \to Q\bar{Q}(n)]\langle 0 \mid \mathcal{O}_n^{J/\psi(\Upsilon)} \mid 0\rangle \quad (3)$$

The first term in the right hand side of Eq.(3) was given in [15] that describes the production of heavy quark and anti-quark pair in a definite quantum state and it can be calculated in order α_s. Spin, orbital angular momentum and color quantum numbers are denoted with n. After forming the heavy quark pair, its quantum numbers will be readjusted to form a color singlet quarkonium state by emitting or absorbing soft gluons. This process is absorbed in $\langle 0 \mid \mathcal{O}_n^{J/\psi(\Upsilon)} \mid 0\rangle$ (LDME) which is nonperturbative. All possible configurations of heavy quark pair in different quantum states are taken into account for quarkonium production which is represented with summation over n in Eq.(3). In line with Ref. [22, 23], we consider only the color octet states $^1S_0$, $^3P_0$ and $^3P_2$ which have dominant contribution in charmonium and bottomonium production. The LDME numerical values of these color octet states are extracted in Ref.[24, 25, 26], which are tabulated in [15]. After integrating w.r.t x_a, x_b and $\mathbf{k}_{\perp b}$ in Eq.(1) and following the steps in Ref. [15], one can obtain the differential cross section as

$$\frac{d\sigma^{ff+hh}}{dyd^2\mathbf{p}_T} = \frac{d\sigma^{ff}}{dyd^2\mathbf{p}_T} + \frac{d\sigma^{hh}}{dyd^2\mathbf{p}_T}, \quad (4)$$

where

$$\frac{d\sigma^{ff}}{dyd^2\mathbf{p}_T} = \frac{C_n}{s}\int d^2\mathbf{k}_{\perp a} f_1^g(x_a, \mathbf{k}_{\perp a}^2) f_1^g(x_b, \mathbf{k}_{\perp b}^2), \quad (5)$$

$$\frac{d\sigma^{hh}}{dyd^2\mathbf{p}_T} = \frac{C_n}{s}\int d^2\mathbf{k}_{\perp a} w h_1^{\perp g}(x_a, \mathbf{k}_{\perp a}^2) h_1^{\perp g}(x_b, \mathbf{k}_{\perp b}^2), \quad (6)$$

$w = \frac{1}{2M_h^4}\Big[(\mathbf{k}_{\perp a}.\mathbf{k}_{\perp b})^2 - \frac{1}{2}\mathbf{k}_{\perp a}^2\mathbf{k}_{\perp b}^2\Big]$ and $\mathbf{k}_{\perp b} = \mathbf{p}_T - \mathbf{k}_{\perp a}$. The definition of C_n is given in Eq.(6) of Ref. [15]. Here p_T and y are the transverse momentum and rapidity of the quarkonium.

III. EVOLUTION OF TMDS

As per Ref. [14], we assume that the unpolarized and linearly polarized gluon TMDs follow the Gaussian form. In Gaussian parametrization, TMDs are factorized into product of collinear PDFs times exponential factor which is a function of only $k_\perp$ and Gaussian width.

$$f_1^g(x, \mathbf{k}_\perp^2) = f_1^g(x, Q^2)\frac{1}{\pi\langle k_\perp^2\rangle} e^{-\mathbf{k}_\perp^2/\langle k_\perp^2\rangle}, \quad (7)$$

$$h_1^{\perp g}(x, \mathbf{k}_\perp^2) = \frac{M_h^2 f_1^g(x, Q^2)}{\pi\langle k_\perp^2\rangle^2}\frac{2(1-r)}{r} e^{1-\mathbf{k}_\perp^2\frac{1}{r\langle k_\perp^2\rangle}}, \quad (8)$$

where, $f_1^g(x, Q^2)$ is the collinear PDF which follows the DGLAP evolution equation and $r = 2/3$ and $1/3$ [14] values are taken for numerical estimation. The Gaussian widths are $\langle k_\perp^2\rangle = 0.25$ GeV^2 and 1 GeV^2 [14]. In model-I, we do not take any upper limit for $k_{\perp a}$ integration. An upper limit $k_{\max} = \sqrt{\langle k_\perp^2\rangle}$ [27] is considered for $k_{\perp a}$ integration in model-II. The analytical expressions of differential cross sections for model-I and model-II are given in Sec-(III) [15]. As pointed out in Ref.[4], in order to explain high p_T spectrum one has to consider the full TMD evolution approach which was derived in impact parameter space ($b_\perp$). The Fourier transformations of gluon-gluon correlator in $b_\perp$ and $k_\perp$ space are

$$\Phi(x, \mathbf{b}_\perp) = \int d^2\mathbf{k}_\perp e^{-i\mathbf{k}_\perp.\mathbf{b}_\perp}\Phi(x, \mathbf{k}_\perp), \quad (9)$$

$$\Phi(x, \mathbf{k}_\perp) = \frac{1}{(2\pi)^2}\int d^2\mathbf{b}_\perp e^{i\mathbf{k}_\perp.\mathbf{b}_\perp}\Phi(x, \mathbf{b}_\perp). \quad (10)$$

The gluon correlator in $b_\perp$ space is given by [12]

$$\Phi^g(x, \mathbf{b}_\perp) = \frac{1}{2x}\Big\{g_T^{\mu\nu} f_1^g(x, \mathbf{b}_\perp^2) - \Big(\frac{2b_\perp^\mu b_\perp^\nu}{b_\perp^2} - g_T^{\mu\nu}\Big) h_1^{\perp g}(x, \mathbf{b}_\perp^2)\Big\}. \quad (11)$$

In TMD evolution approach, TMDs depend on both renormalization scale μ and auxiliary scale ζ which was introduced to regularize the rapidity divergences. Renormalization group (RG) and Collins-Soper (CS) equations are obtained by taking scale evolution w.r.t the scales μ and ζ. After solving these equations one obtains the TMD evolution expressions of TMDs in $b_\perp$ space [17, 28, 29]. The differential cross section expressions of Eq.(4) in TMD evolution approach are given by [15]

$$\frac{d^2\sigma^{ff}}{dydp_T^2} = \frac{C_n}{2s}\int_0^\infty b_\perp db_\perp J_0(p_T b_\perp) f_1^g(x_a, c/b_*) \times f_1^g(x_b, c/b_*) R_{\rm pert} R_{\rm NP}, \quad (12)$$

and

$$\frac{d^2\sigma^{hh}}{dydp_T^2} = \frac{C_n C_A^2}{2s\pi^2}\int_0^\infty b_\perp db_\perp J_0(p_T b_\perp)\alpha_s^2(c/b_*) \times \int_{x_a}^1 \frac{dx_1}{x_1}\left(\frac{x_1}{x_a}-1\right) f_1^g(x_1,c/b_*) \times \int_{x_b}^1 \frac{dx_2}{x_2}\left(\frac{x_2}{x_b}-1\right) f_1^g(x_2,c/b_*) R_{\rm pert} R_{\rm NP} \tag{13}$$

where $R_{\rm pert}$ and $R_{\rm NP}$ are the perturbative and nonperturbative parts of the evolution kernel.

$$R_{\rm pert} = \exp\left\{-2\int_{c/b_*}^{Q}\frac{d\mu}{\mu}\left(A\log\left(\frac{Q^2}{\mu^2}\right)+B\right)\right\}$$

$$R_{\rm NP} = \exp\left\{-\left[0.184\log\frac{Q}{2Q_0}+0.332\right]b_\perp^2\right\}$$

Here A and B are the anomalous dimensions of the evolution kernel and TMDs respectively and these have perturbative expansion [15]. We used the b_* prescription to avoid the Landau poles by freezing the scale as $b_*(b_\perp) = \frac{b_\perp}{\sqrt{1+\left(\frac{b_\perp}{b_{\rm max}}\right)^2}}$. In the nonperturbative regime where $b_\perp$ is very large, the evolution kernel cannot be calculated using perturbation theory. Hence, the evolution kernel in this regime is modeled as $R_{\rm NP}$ [28]. We have considered the same nonperturbative factor $R_{\rm NP}$ for both unpolarized and linearly polarized gluon TMDs.

IV. NUMERICAL RESULTS

We calculated the transverse momentum (p_T) distribution of J/ψ and $\Upsilon(1S)$ in unpolarized proton-proton collision at LHC ($\sqrt{s} = 7$ TeV), RHIC ($\sqrt{s} = 500$ GeV) and AFTER ($\sqrt{s} = 115$ GeV) energies. Quarkonium production rates are estimated using NRQCD version COM within TMD factorization framework. Color octet states such as $^1S_0$, $^3P_0$ and $^3P_2$ of initially produced heavy quark pair are taken into account for quarkonium production. The masses of J/ψ and $\Upsilon(1S)$ are considered 3.096 and 9.398 GeV respectively. $m_c = 1.5$ GeV and $m_b = 4.8$ GeV are taken for charm and bottom quark masses respectively. MSTW2008 [39] is used for gluon PDFs. $Q = M$ (quarkonium mass) is considered for scale of the gluon PDFs in DGLAP evolution. Quarkonium p_T distribution is obtained by integrating rapidity in the range of $y \in [2.0, 4.5]$, $y \in [-3.0, 3.0]$ and $y \in [-0.5, 0.5]$ for LHCb, RHIC and AFTER respectively. The convention in the figures as follows. "ff"and "ff+hh"represent the quarkonium distribution obtained by taking into account only unpolarized gluons and linearly polarized plus unpolarized gluons respectively.

FIG.1 represents the p_T spectrum of J/ψ and $\Upsilon(1S)$ which is estimated in COM. In FIG.1, the cross section

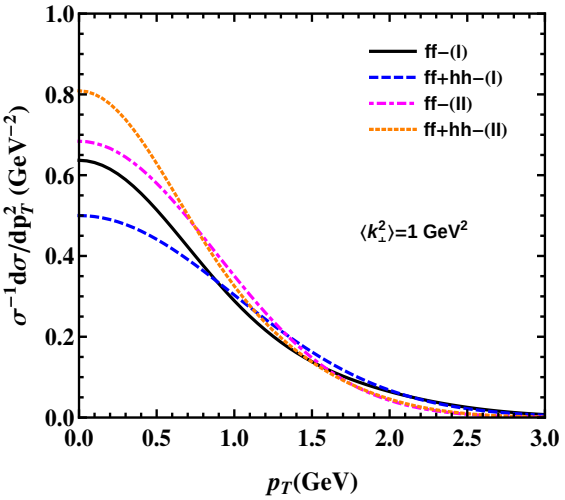

(a)

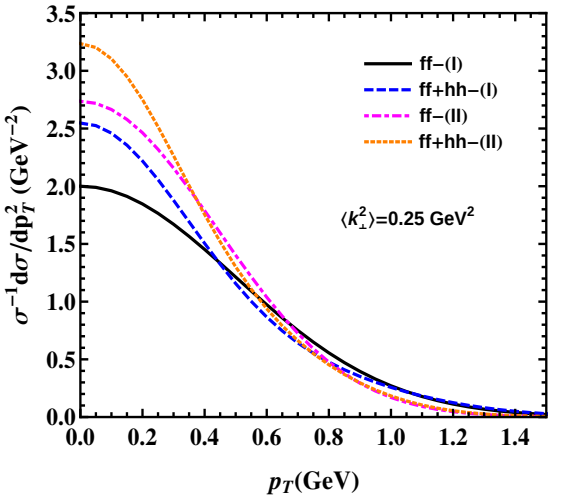

(b)

FIG. 1. (color online) Differential cross section (normalized) of J/ψ and $\Upsilon(1S)$ production in $pp \to J/\psi(\Upsilon(1S)) + X$ at LHCb ($\sqrt{s} = 7$ TeV), RHIC ($\sqrt{s} = 500$ GeV) and AFTER ($\sqrt{s} = 115$ GeV) energies using DGLAP evolution approach for (a) $\langle k_\perp^2\rangle = 1$ GeV^2 and (b) $\langle k_\perp^2\rangle = 0.25$ GeV^2 at $r = \frac{2}{3}$. The solid (ff-(I)) and dot dashed (ff-(II)) lines are obtained by considering unpolarized gluons in Model-I and Model-II respectively. The dashed (ff+hh-(I)) and tiny dashed (ff+hh-(II)) lines are obtained by taking into account unpolarized gluons plus linearly polarized gluons in Model-I and Model-II respectively. See the text for ranges of rapidity integration [15].

differential in p_T is normalized with total cross section as a result we obtain the p_T spectrum which is independent of center of mass energy and quarkonium mass. The obtained p_T spectrum in DGLAP evolution approach in model-I and model-II are compared in FIG.1 at $r = 2/3$. The quarkonium p_T spectrum has been modulated significantly by taking into consideration of linearly polarized gluons along with the unpolarized gluons in the scattering process. The effect of linearly polarized gluons is more in model-II compared to model-I. In FIG.2, the estimated

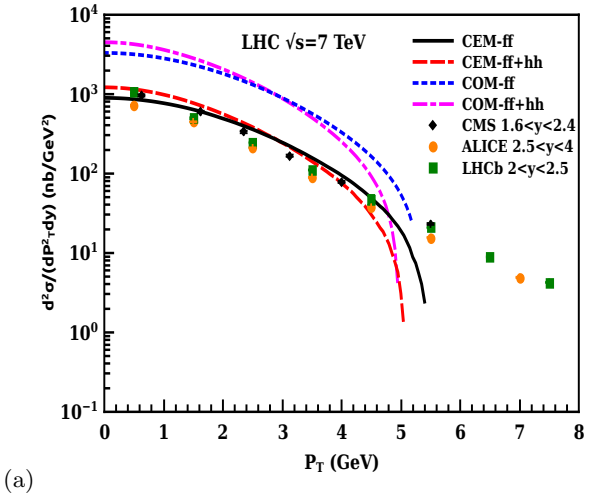

(a)

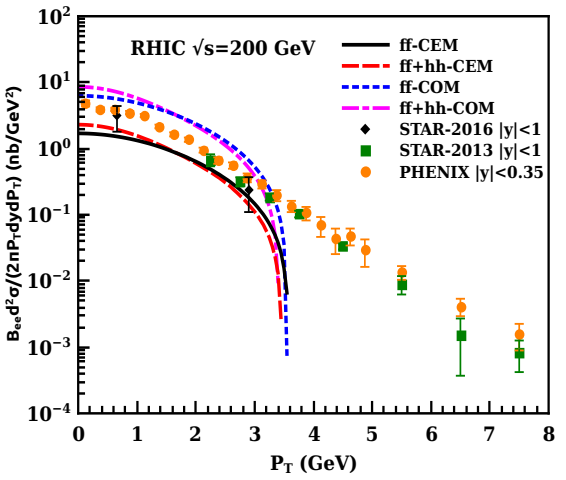

(b)

FIG. 2. (color online). Differential cross section of J/ψ at (a) LHCb ($\sqrt{s}$ = 7 TeV) and (b) RHIC ($\sqrt{s}$ = 200 GeV) as function of p_T in $pp \to J/\psi + X$ using TMD evolution approach. Data are taken from [30, 31, 32] and [33, 34, 35] for LHC and RHIC respectively. The rapidity in the range $2.0 < y < 2.5$ and $-0.35 < y < 0.35$ is chosen for LHCb and RHIC energies respectively [15].

p_T spectrum of J/ψ in TMD evolution approach at LHCb and RHIC energies in COM and CEM are compared with data. Experimental data is taken from Ref. [30, 31, 32] and Ref. [33, 34, 35] for LHCb and RHIC experiments respectively. In FIG.3, p_T spectrum of Υ(1S) using TMD evolution approach in COM and CEM is compared with data [36, 37, 38]. The production rates are in good accuracy with data up to low p_T for both J/ψ and Υ(1S), however, COM is slightly over estimated. In FIG.2 and FIG.3, B_{ee} (0.0594) and $B_{\mu\mu}$ (0.0248) are the branching ratios of $J/\psi \to e^+e^-$ and $\Upsilon(1S) \to \mu^+\mu^-$ channels respectively. J/ψ and Υ(1S) states can be produced from higher mass excited states. However, we have considered only the direct production of quarkonium in this article. In general, LO calculation is insufficient to explain full p_T spectrum. It may be possible to explain high p_T spectrum by adding NLO calculation with LO.

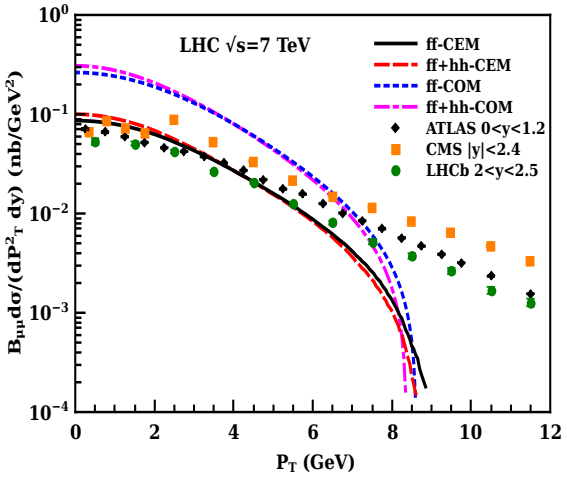

FIG. 3. (color online). Differential cross section of Υ(1S) at LHCb ($\sqrt{s}$ = 7 TeV) as function of p_T in $pp \to \Upsilon(1S) + X$ using TMD evolution approach. Data are taken from [36, 37, 38]. The rapidity in the range $2.0 < y < 2.5$ is chosen [15].

V. CONCLUSION

We studied the transverse momentum (p_T) distribution of J/ψ and Υ(1S) in unpolarized proton-proton collision within TMD factorization formalism. NRQCD based color octet model is employed to estimate the quarkonium production rates. The quarkonium p_T spectrum has been modulated by the presence of linearly polarized gluons inside unpolarized proton and is in good agreement with LHCb and RHIC data. Hence, quarkonium production offers a good possibility to probe both unpolarized and linearly polarized gluon TMDs.

ACKNOWLEDGEMENT

SR acknowledges IIT Bombay and spin symposium organizers for financial support to attend the 22nd International Spin Symposium, 2016, UIUC.

[1] P. J. Mulders and J. Rodrigues, Phys. Rev. **D63**, 094021 (2001), hep-ph/0009343.

[2] R. Angeles-Martinez et al., Acta Phys. Polon. **B46**, 2501 (2015), 1507.05267.

[3] S. Meissner, A. Metz, and K. Goeke, Phys. Rev. **D76**, 034002 (2007), hep-ph/0703176.
[4] S. Melis, EPJ Web Conf. **85**, 01001 (2015), 1412.1719.
[5] D. W. Sivers, Phys. Rev. **D41**, 83 (1990).
[6] C. Pisano, D. Boer, S. J. Brodsky, M. G. A. Buffing, and P. J. Mulders, JHEP **10**, 024 (2013), 1307.3417.
[7] W. J. den Dunnen, J. P. Lansberg, C. Pisano, and M. Schlegel, Phys. Rev. Lett. **112**, 212001 (2014), 1401.7611.
[8] J.-W. Qiu, M. Schlegel, and W. Vogelsang, Phys. Rev. Lett. **107**, 062001 (2011), 1103.3861.
[9] D. Boer, W. J. den Dunnen, C. Pisano, M. Schlegel, and W. Vogelsang, Phys. Rev. Lett. **108**, 032002 (2012), 1109.1444.
[10] D. Boer, W. J. den Dunnen, C. Pisano, and M. Schlegel, Phys. Rev. Lett. **111**, 032002 (2013), 1304.2654.
[11] M. G. Echevarria, T. Kasemets, P. J. Mulders, and C. Pisano, JHEP **07**, 158 (2015), 1502.05354.
[12] D. Boer and W. J. den Dunnen, Nucl. Phys. **B886**, 421 (2014), 1404.6753.
[13] D. Boer and C. Pisano, Phys. Rev. **D91**, 074024 (2015), 1412.5556.
[14] D. Boer and C. Pisano, Phys. Rev. **D86**, 094007 (2012), 1208.3642.
[15] A. Mukherjee and S. Rajesh (2016), 1611.05974.
[16] A. Mukherjee and S. Rajesh, Phys. Rev. **D93**, 054018 (2016), 1511.04319.
[17] J. Collins, *Foundations of perturbative QCD* (Cambridge University Press, 2013), URL http://www.cambridge.org/de/knowledge/isbn/item5756723.
[18] J. F. Amundson, O. J. P. Eboli, E. M. Gregores, and F. Halzen, Phys. Lett. **B372**, 127 (1996), hep-ph/9512248.
[19] J. F. Amundson, O. J. P. Eboli, E. M. Gregores, and F. Halzen, Phys. Lett. **B390**, 323 (1997), hep-ph/9605295.
[20] G. T. Bodwin, E. Braaten, and G. P. Lepage, Phys. Rev. **D51**, 1125 (1995), [Erratum: Phys. Rev.D55,5853(1997)], hep-ph/9407339.
[21] G. T. Bodwin, E. Braaten, and G. P. Lepage, Phys. Rev. **D46**, R1914 (1992), hep-lat/9205006.
[22] S. Fleming and I. Maksymyk, Phys. Rev. **D54**, 3608 (1996), hep-ph/9512320.
[23] F. Cooper, M. X. Liu, and G. C. Nayak, Phys. Rev. Lett. **93**, 171801 (2004), hep-ph/0402219.
[24] Y.-Q. Ma and R. Venugopalan, Phys. Rev. Lett. **113**, 192301 (2014), 1408.4075.
[25] K.-T. Chao, Y.-Q. Ma, H.-S. Shao, K. Wang, and Y.-J. Zhang, Phys. Rev. Lett. **108**, 242004 (2012), 1201.2675.
[26] R. Sharma and I. Vitev, Phys. Rev. **C87**, 044905 (2013), 1203.0329.
[27] M. Anselmino, M. Boglione, U. D'Alesio, A. Kotzinian, S. Melis, F. Murgia, A. Prokudin, and C. Turk, Eur. Phys. J. **A39**, 89 (2009), 0805.2677.
[28] S. M. Aybat and T. C. Rogers, Phys. Rev. **D83**, 114042 (2011), 1101.5057.
[29] S. M. Aybat, A. Prokudin, and T. C. Rogers, Phys. Rev. Lett. **108**, 242003 (2012), 1112.4423.
[30] R. Aaij et al. (LHCb), Eur. Phys. J. **C71**, 1645 (2011), 1103.0423.
[31] V. Khachatryan et al. (CMS), Eur. Phys. J. **C71**, 1575 (2011), 1011.4193.
[32] B. B. Abelev et al. (ALICE), Eur. Phys. J. **C74**, 2974 (2014), 1403.3648.
[33] L. Adamczyk et al. (STAR), Phys. Lett. **B722**, 55 (2013), 1208.2736.
[34] L. Adamczyk et al. (STAR), Phys. Rev. **C93**, 064904 (2016), 1602.02212.
[35] A. Adare et al. (PHENIX), Phys. Rev. **D82**, 012001 (2010), 0912.2082.
[36] R. Aaij et al. (LHCb), Eur. Phys. J. **C72**, 2025 (2012), 1202.6579.
[37] S. Chatrchyan et al. (CMS), Phys. Lett. **B727**, 101 (2013), 1303.5900.
[38] G. Aad et al. (ATLAS), Phys. Rev. **D87**, 052004 (2013), 1211.7255.
[39] A. D. Martin, W. J. Stirling, R. S. Thorne, and G. Watt, Eur. Phys. J. **C63**, 189 (2009), 0901.0002.